

PHOTOIMAGEABLE THICK-FILM MICROWAVE STRUCTURES UP TO 18 GHz

B. DZIURDZIA¹, Z. MAGOŃSKI¹, S. NOWAK², M. CIEŻ², W. GREGORCZYK³, W. NIEMYJSKI⁴

¹Academy of Mining and Metallurgy, AGH, al. Mickiewicza 30, 30-059 Kraków, Poland,

²Institute of Electron Technology, Department in Kraków, ul. Zabłocie 39, 30-701 Kraków, Poland,

³Telecommunications Research Institute, ul. Poligonowa 30, 04-051 Warszawa, Poland,

⁴Microwave Systems Poland, ul. Budowlanych 48, 80-298 Gdańsk, Poland

Received December 31, 2003; accepted January 26, 2004; published February 3, 2004

ABSTRACT

The increasing interest in new wireless applications is creating demand for low cost, high performance microwave hybrid circuits. Offering the inherent advantages of thick-film technology such as low manufacturing costs and feasibility for mass production, recent improvements in thick film materials and processing techniques broadens the frequency range where ceramic thick-film circuits can be used and allow current thick-film technology to reach beyond its previous limitations and enter the domain reserved in the past for thin film technology. This paper discusses the advanced thick-film technique called photoimageable thick-film technology that uses photosensitive conductor and dielectric pastes and photoimaging as a method of patterning for manufacturing microwave hybrids operating in the frequency range up to 18 GHz.

1. Introduction

Until now thin film technology has been most commonly used in manufacturing microwave hybrids. However, an often overlooked option for thin film technology is thick-film technology especially in a lower range of microwave spectrum. Thick-film technology offers improvement of circuit thermal dissipation and environmental robustness, low cost and feasibility to high volume production that is an important factor in the time of explosive growth of wireless communication. Moving the useful electromagnetic spectrum into higher regions of frequency implies searching for more precise method of patterning which results in enhanced circuit performance with dense interconnects, smooth surfaces, rectangular walls and sharp edges of microwave structures.

This is beyond capabilities of traditional screen printing even when fine screens and advanced fritless pastes are used and that is the reason why photoimageable thick-film technology is emerging on the stage of modern technologies [1–4].

2. Photoimageable thick-film technology

2.1. Photoimaging process

Photoimageable thick-film technology is a combination of conventional thick-film technology with

some processes typical for thin film technology. The first manufacturing step is a deposition of the photosensitive paste on a substrate by blank screen printing. The paste is levelled at room temperature and then dried at 80°C. The dried layer is exposed to UV light through a negative photomask to form a latent image which afterwards is developed in a development processor using appropriate development solution. At the end, the developed pattern is fired in the furnace typical for thick-films [1]. Figure 1 shows a processing sequence for photoimageable conductors in comparison to etching of fired thick-film conductors and reveals the simplicity of photoimaging.

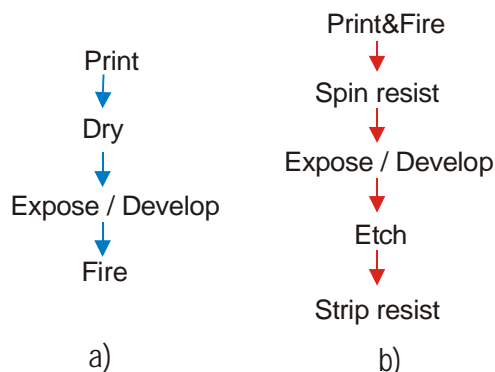


Fig. 1. a) Photoimaging sequence, b) etching sequence.

In contrast to standard thick-film process, the photoimageable process separates printing and pattern generation allowing independent optimisation of these two manufacturing steps. Photosensitive pastes are designed to form very smooth surface, free of pinholes and other defects after printing. That is the job of exposure and development process to provide high resolution and good quality of the pattern. Photoimaging makes available 50 μm lines and spaces with accuracy of 5 μm and smooth, well defined, near-vertical edge features, while dielectrics resolve 75 μm vias on a 125 μm pitch. The standard resolution for traditional thick-film technology is 150 μm line/200 μm space with accuracy 25 μm and 250 μm via diameter on a 500 μm pitch [1].

2.2. Photoimageable conductors and dielectrics

Photoimageable technology requires special thick-film materials. Photosensitive pastes contain a photoinitiator which during UV exposure absorbs light and starts polymerization of the acrylic monomers turning them into photopolymers. Photopolymers harden in the exposed areas while the parts of the layer in unexposed areas are easily dissolved and removed under the development solution.

Table 1. Fodel conductor Ag 6778 [1]

Parameter	Fodel 6050
Dielectric constant (at 10 MHz)	7 ÷ 9
Dissipation factor (at 10 MHz)	0.004
Insulation resistance	> 10 ¹¹ Ω
Breakdown voltage (per 25 μm)	> 1000 V
Thickness (4 prints, 2 firings)	40 ÷ 45 μm
Via diameter resolution	75 μm
Fired thickness	8 ÷ 10 μm
Screen printing	Stainless screen 200 mesh
Leveling	10 ÷ 15 min. at room temperature
Drying	20 ÷ 25 min. at 80°C
Exposure	1000 W, Hg or Hg/Xe collimated light source, wavelength 365 nm to 400 nm, exposure energy 18 ÷ 35 mJ/cm ² , exposure time for 14 ÷ 18 μm dried thickness 1.5 ÷ 3 s
Development	1% Na ₂ CO ₃ at 30°C
Rinse	With water immediately after development
Firing	850°C, 60 min.

Photoimageable conductors and dielectrics of several manufacturers such as Du Pont, ESL, Heraeus and Hybridas are available on the market. In

experiments reported in this paper silver photoimageable conductor Fodel Ag 6778 and dielectric Fodel 6050 were used and their basic properties are collected in Table 1 and Table 2.

Table 2. Fodel 6050 dielectric [1]

Parameter	Fodel Ag 6778
Metallurgy	silver
Substrate	96% Al ₂ O ₃ , 99% Al ₂ O ₃ , Green Tape, Fodel 6050 dielectric
Line resolution	50 μm line/50 μm space
Resistivity	2.5 m Ω /sq.
Fired thickness	8 ÷ 10 μm
Screen printing	Stainless screen 325 ÷ 400 mesh
Leveling	10 ÷ 15 min. at room temperature
Drying	20 ÷ 25 min. at 80°C
Exposure	1000 W, Hg or Hg/Xe collimated light source, wavelength 365 nm to 400 nm, exposure energy 280 ÷ 840 mJ/cm ² , exposure time for 14 ÷ 18 μm dried thickness 20 ÷ 100 s
Development	1% Na ₂ CO ₃ at 30°C
Rinse	With water immediately after development
Firing	850°C, 60 min.

Photoimageable thick film conductors and dielectrics have post-fired properties similar to standard thick-film materials because all photosensitive ingredients are being removed during the firing process. In all areas where Du Pont and ESL pastes are printed, dried, exposed and developed the safe yellow light should be used to prevent accidental polymerization.

2.3. Exposure unit

The photoimageable process requires a typical technological line for thick-films completed by the exposure and development units.

The exposure unit used in reported below experiments (Fig. 2) was adapted for photoimaging of thick-films on the basis of the exposure unit typical for processing thin films [5]. During rearrangement, it was equipped with a new high pressure mercury lamp of power 500 W with improved efficient cooling, ignition and shutter driving systems. The lamp emits UV light in the wavelength range from 365 nm to 420 nm. The light beam is collimated by the set of condenser lens and travels in a horizontal path towards the exposure mirror where it is reflected down to a substrate. The unit is equipped with a mask and a substrate alignment system that permits setting the mask over



Fig. 2. Exposure unit – a general view.

the substrate under control of a split-field microscope. The condenser lens are protected by an efficient infra-red cut-off filter that is additionally cooled with a stream of decompressing nitrogen.

Photo-tools used were film masks - right reading, image down, negatives.

2.4. Development unit

The development unit used in experiments is on-custom design [5] that enables developing of the exposed pattern in mist of 1% aqueous solution of Na_2CO_3 . The substrate rotates horizontally on a rotary station at a speed ranging from 100 to 250 rpm. Development solution is changed into a fine mist by the ultrasonic generator and blown off through the flat nozzle using nitrogen as a carrier medium. Passing through the slot of the nozzle, the mist gains some impact energy and striking at the substrate removes unexposed soluble parts of the thick film layer. Rotation supports removing the remains. The mist of deionised water produced by another ultrasonic generator stops the process of development. After development the substrate is dried while rotating at higher speed. Figure 3 shows the



Fig. 3. Development unit – a general view.

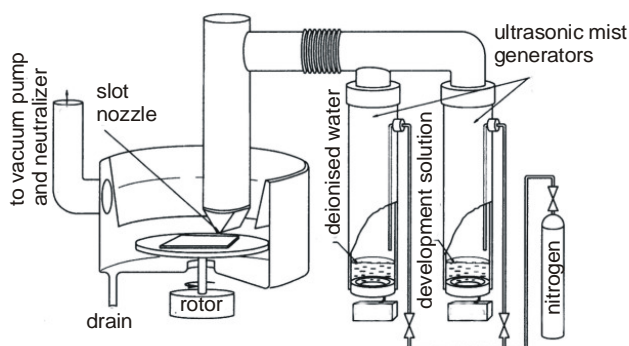


Fig. 4. Development unit – a principle of operation.

general view of the development unit and Fig. 4 presents the principle of its operation.

2.5. Photoimaging process parameters

2.5.1. Printing & drying

The Fodel Silver Ag 6778 or Fodel dielectric 6050 were applied to the alumina substrates (96% Al_2O_3) by blanket screen printing through stainless steel screen of 325 mesh for the conductor and 200 mesh for the dielectric, respectively. The wet print was leveled for 5 ÷ 10 min. at room temperature and then dried in a ventilated box oven for 25+/-5 min. at 80+/-1°C.

Both temperature and time of drying were strictly controlled to prevent deactivation of a photosensitive system of the layer. In order to obtain the recommended by the manufacturer fired thickness of the dielectric layer equal to 40+/-2 μm , the process of printing and drying were doubled according to a sequence: [(PRINT/DRY, PRINT/DRY) / FIRE] x 2.

2.5.2. Exposure

The dried conductor or dielectric were exposed in the exposure unit through negative film photomasks. The time of exposure providing satisfactory line and vias resolution was experimentally adjusted with the appropriate development time and was established at level of 60 s for the Fodel conductor and 3 s for the Fodel dielectric.

2.5.3. Development

Development process was carried out using the mist of the 1% aqueous Na_2CO_3 development solution. The development time of about 15 s was established to obtain the resolution 50 μm line/50 μm space and vias resolution of 75 μm in diameter.

2.5.4. Firing

Firing of Fodel conductor and dielectric was performed in a belt furnace typical for thick films

during a 60 min. firing cycle with a peak temperature of 850°C for 10 min.

3. Microwave circuit designs

To show the practical application of photo-imageable technology for performing microwave circuits some test structures such as:

- the ring resonator of fundamental resonance frequency 3.6 GHz,
 - the band-pass filters of centre frequency 1 GHz, 18 GHz,
 - the broadside coupler of frequency 7.5 GHz,
- have been designed and fabricated.

Figure 5 shows the test samples.

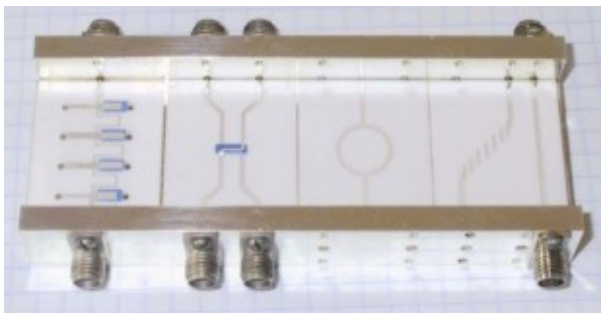


Fig. 5. Photoimageable microwave hybrids.

Additionally, the set of test lines of width 30, 50, 75, 100, 125, 150 μm and the set of test vias of diameters of 75, 100, 125, 150 μm have been designed to establish the line resolution and vias resolution achievable for the given experimental facilities.

3.1. Ring resonator of fundamental resonance frequency 3.6 GHz

Microstrip ring resonator was used to evaluate effective dielectric constant ϵ_{eff} and quality factor Q of dielectric/metal systems.

The ring configuration was chosen to eliminate end effect corrections required for linear resonators and to minimize parasitic losses due to radiation and surface waves.

Effective dielectric constant, which includes a contribution from the air above the part, was obtained from resonant frequency measurements.

Resonance occurs when the ring circumference is equal to the guide wavelength. In a microstrip configuration the effective dielectric constant is obtained from the equation [6]:

$$\epsilon_{\text{eff}} = \left(\frac{cn}{\pi D f_{\text{res}}} \right)^2 \quad (1)$$

where c is the speed of light, n is the order of the harmonic, D is the ring diameter and f_{res} is the resonant frequency.

Power consumption becomes a major concern in portable wireless devices. This property is characterized by quality factor Q which is the system property relating to the use of power supplied to the device. It is defined as the ratio of energy stored to energy lost per cycle. For a ring resonator, Q of the system can be obtained from [6]:

$$Q_L = \frac{f_{\text{res}}}{\Delta f_{3\text{dB}}} \quad (2)$$

where $\Delta f_{3\text{dB}}$ is the 3-dB frequency range and f_{res} is the resonant frequency.

The quality factor Q determined in this way is for the ring resonators the quality factor under load Q_L which varies with gap separation. To get unloaded quality factor Q_U , the following correction is needed [6]:

$$Q_U = \frac{Q_L}{1 - 10^{(-L/20)}} \quad (3)$$

where L is the insertion loss maximum in dB.

Attenuation α_g per guide wavelength λ_g for the metal/ceramic system can be calculated using [5]:

$$\alpha_g = \frac{20\pi \log_{10}(e)}{Q_U} [\text{dB}/\lambda_g]. \quad (4)$$

The ring resonator design (Fig. 6) and simulated transmission (S_{21}) and reflection (S_{11}) characteristics were created by Genesis 8.11 software taking into account the following assumptions for the alumina substrate and silver metallization:

- $h = 0.635$ mm (thickness of a substrate),
- $\epsilon_r = 9.6$ (dielectric constant of a substrate),
- $\text{tg}\delta = 0.004$ (tangent loss of a substrate),
- $t = 0.008$ mm (thickness of metallization).

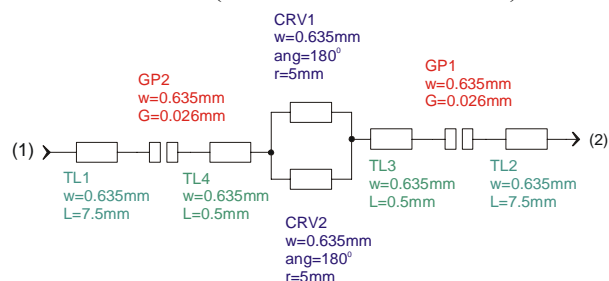


Fig. 6. Ring resonator created by Genesis 8.11 software.

Figure 6 shows the layout of a ring resonator, Fig. 7 its simulated transmission and reflection characteristics, and Fig. 8 is a photo of the microwave structure.

3.2. Bandpass filter 1 GHz

Bandpass filters are essential components in communication systems. Based on the full-wave electromagnetic simulation tools, a bandpass filter of centre frequency 1 GHz, 3 dB-bandwidth 180 MHz and attenuation in the passband of 1.65 dB was designed. The filter structure (Fig. 9) is composed of quarter-wave transmission lines shunted by

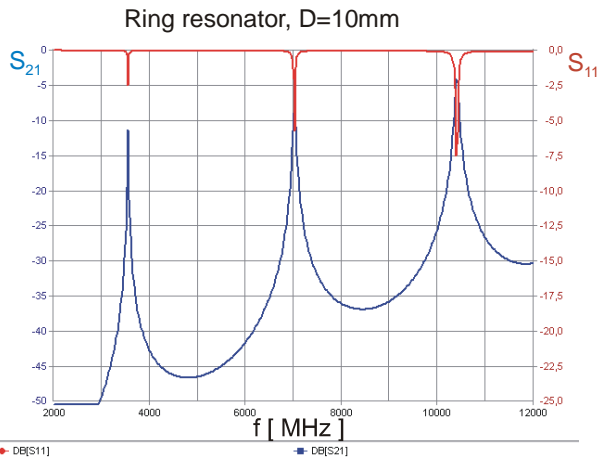


Fig. 7. Simulated transmission (S_{21}) and reflection (S_{11}) characteristics of the ring resonator of diameter 10 mm.

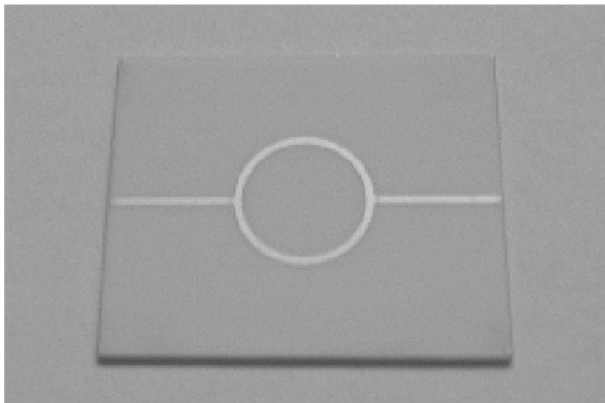


Fig. 8. Photoimageable thick-film ring resonator of diameter 10 mm.

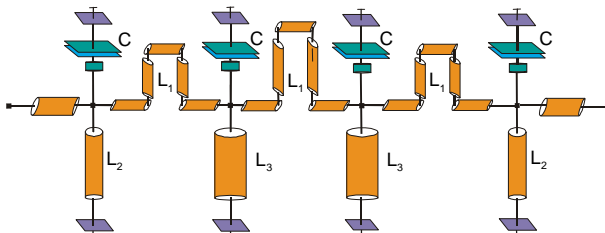


Fig. 9. Schematic of the 1 GHz bandpass filter.

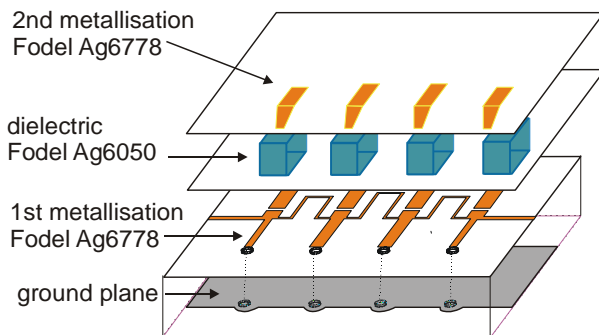


Fig. 10. Details of filter implementation in thick-film.

stub inductors and distributed capacitors connected with the ground plane through via holes in alumina substrate. The physical realization of the filter structure is shown in Figs. 10, 11 and its simulated characteristics in Fig. 12.

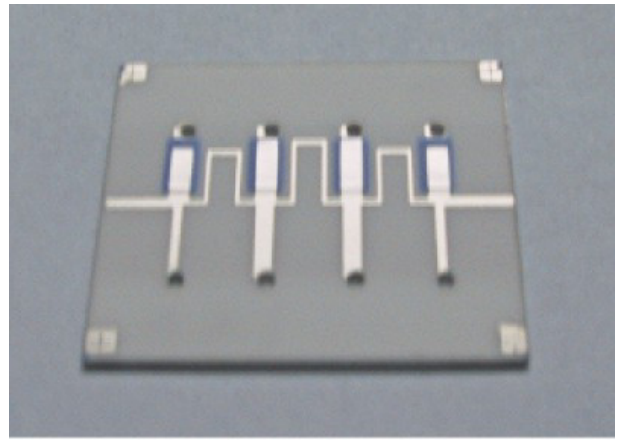


Fig. 11. Photoimageable thick-film bandpass filter 1 GHz.

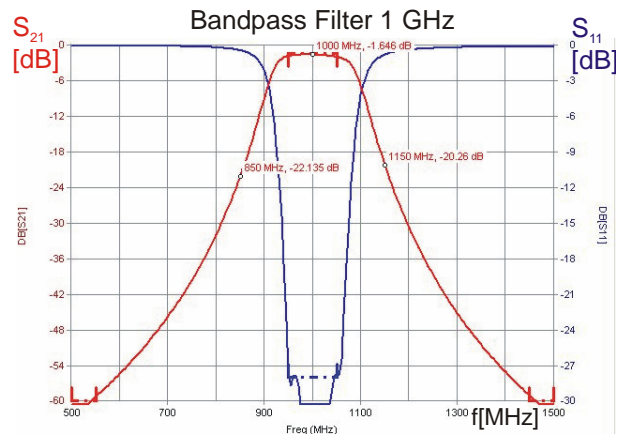


Fig. 12. Simulated transmission (S_{21}) and reflection (S_{11}).

3.3. Bandpass filter 18 GHz

Bandpass filters of center frequency 18 GHz is the edge-coupled filter that consists of 8 resonators. The filter attenuation in the passband is equal to 1.2dB and the 3-dB frequency range 2.5 GHz.

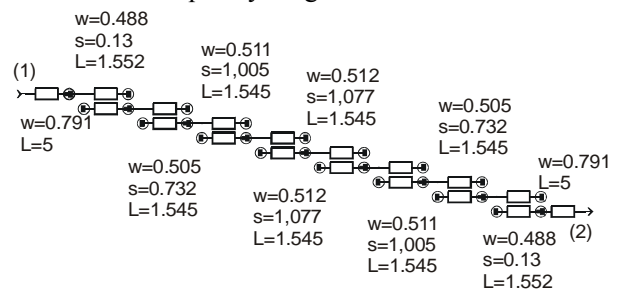


Fig. 13. Bandpass filter 18 GHz created by Genesis 8.11.

Figure 13 shows the filter layout, Fig.14 the simulated characteristics and Fig. 15 the filter photo.

3.4. 3-dB Quadrature hybrid coupler

Couplers are commonly used in many microwave devices. There are two configurations of couplers: side-coupled and broadside-coupled. The characteristic feature of a broadside coupler is, that it is composed of two lines one over another and

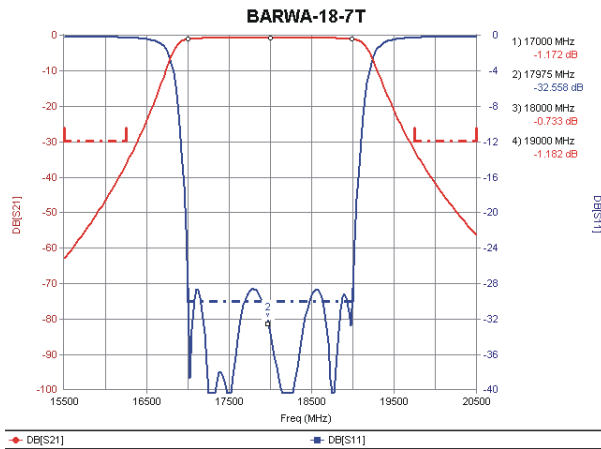


Fig. 14. Simulated transmission (S_{21}) and reflection (S_{11}) characteristics of the 18 GHz filter.

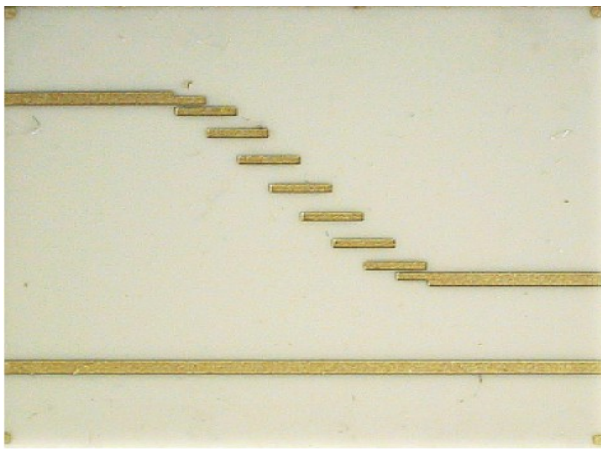


Fig. 15. Photoimageable thick-film bandpass filter 18 GHz.

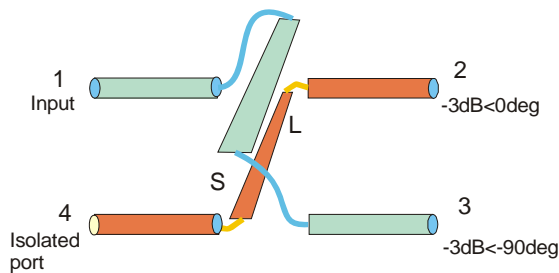


Fig. 16. Schematic of a quadrature hybrid coupler.

between them there is a dielectric material. In a side-coupled device the coupled lines are parallel in X-Y plane. If two outputs of a broadside coupler are equal in amplitude but separated from one another by a constant 90 deg phase, it is called a quadrature hybrid coupler. Figure 16 shows a schematic of a quadrature hybrid coupler.

The microwave energy is applied to port 1 and equally split at ports 2 and 3 with -3dB attenuation. There is also a 90 deg difference in phase between ports 2 and 3. Ports 1 and 4 are isolated and power flowing into port 1 does not appear in port 4. The amount of energy that crosses over between the two circuits depends on the spacing S between microstrips. The length of the coupling area L is set to be one quarter-wavelength at the frequency of

operation. Figure 17 shows the broadside coupler 7.5 GHz implementation into photoimageable technology while Fig. 18 presents its photo.

The simulated characteristics of the coupler are shown in Fig.19.

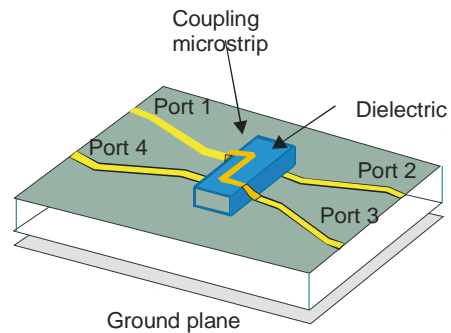


Fig. 17. Photoimageable 7.5 GHz coupler implementation.

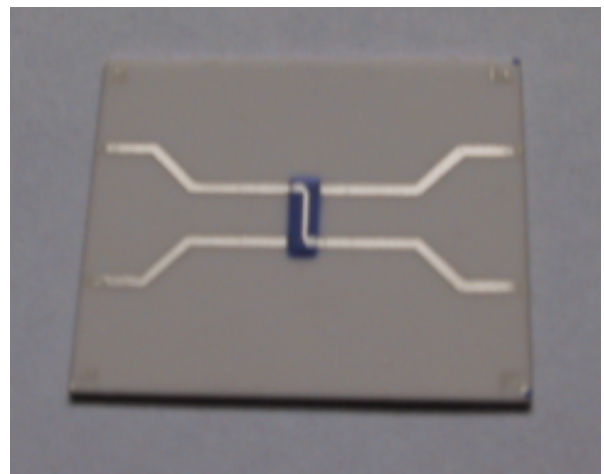


Fig. 18. Photoimageable thick-film broadside coupler 7.5 GHz.

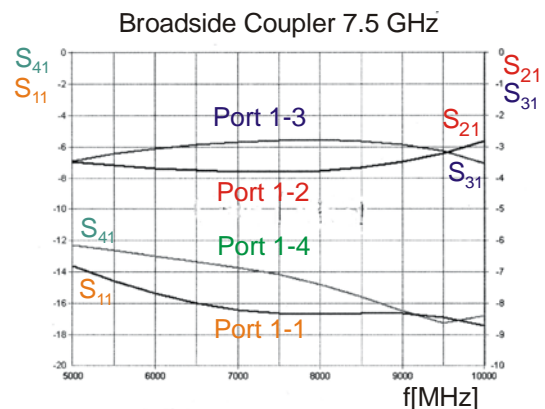


Fig. 19. Simulated characteristics of the broadside coupler 7.5 GHz.

4. Photoimageable implementation of microwave designs

Photoimageable conductor Fodel Ag 6778 and photoimageable dielectric Fodel 6050 were used for deposition on the 96% as-fired alumina substrates of thickness 0.635 mm and dimensions of 30 mm ×

$\times 25$ mm to build single- and double-layer photo-imageable patterns.

The time of exposure of 60 s for the Fodel conductor and 3 s for the Fodel dielectric combined with the development time of 15 s was established to obtain the resolution $50 \mu\text{m}$ line/ $50 \mu\text{m}$ space and via resolution of $75 \mu\text{m}$ in diameter.

Figure 20 shows the SEM photo of the line of width of $50 \mu\text{m}$ ($\times 500$) defined by photoimaging of thick-films. Figure 21 shows the SEM photo of the via of diameter $75 \mu\text{m}$ ($\times 500$) defined by this technique. Figure 22 shows the SEM photo of the edge definition of the Fodel Ag 6778 layer ($\times 1000$).

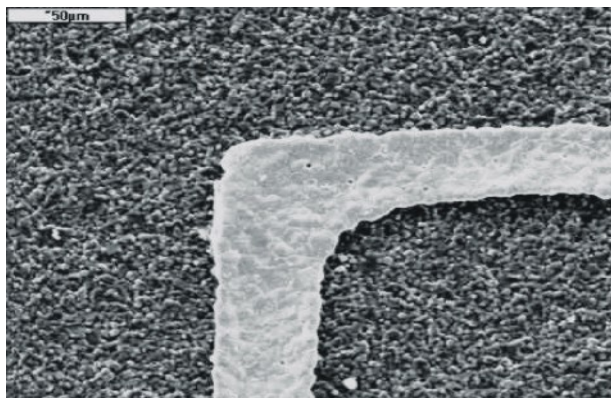


Fig. 20. SEM photo of the line of width of $50 \mu\text{m}$ defined by photoimaging of thick-films, Fodel Ag 6778 ($\times 500$) [7].

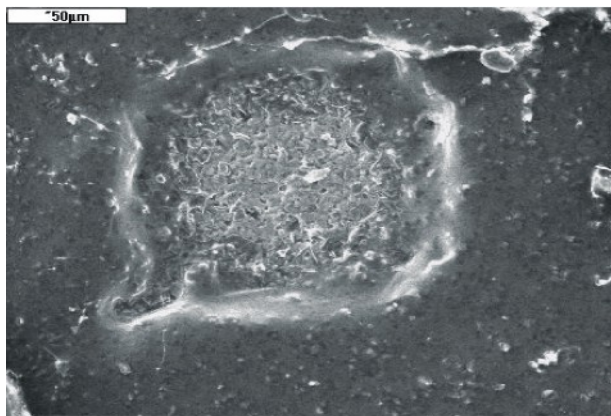


Fig. 21. SEM photo of the via of diameter $75 \mu\text{m}$ defined by photoimaging of thick-films, Fodel Ag 6778 ($\times 500$) [8].

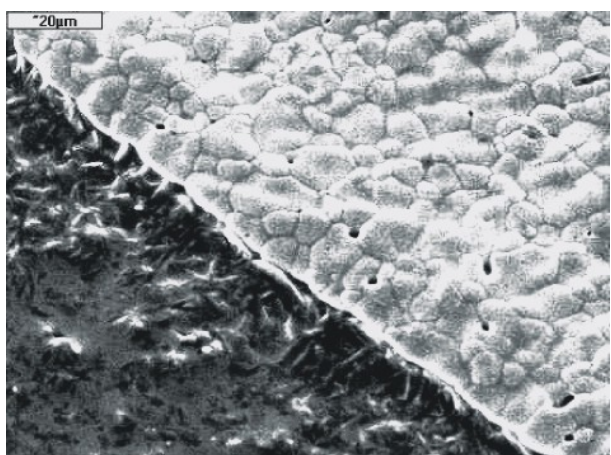


Fig. 22. SEM photo of the surface of the Fodel Ag 6778 layer ($\times 1000$) [7].

The edge curl (Fig. 23) typical for Fodels was observed of about $3 \mu\text{m}$ above the surface layer as

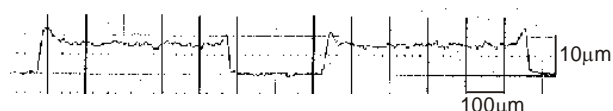


Fig. 23. Cross-section profile of the Fodel Ag 6778 layer [8].

well as a shrinkage of the layer after firing in X-Y plane at a level of $25 \mu\text{m}$. The thickness of the fired layer was equal $8 \mu\text{m}$.

4.1. Ring resonator fabrication and measurements

The ring resonator of the diameter 10 mm, line width 0.635 mm and the gap 0.025 mm between the ring and the connection lines was fabricated using 96% alumina substrates of thickness 0.635 mm and Fodel Silver 6778 conductor. The transmission loss S_{21} of this resonator was measured using HP 8250C Vector Network Analyzer in the frequency range from 1 GHz to 18 GHz (Fig. 24). At the fundamental

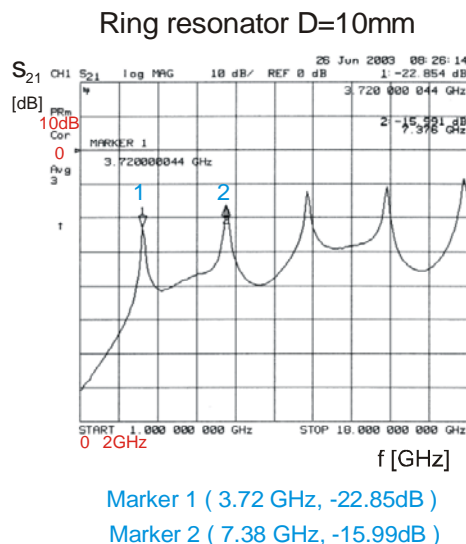


Fig. 24. Transmission coefficient S_{21} of the ring resonator of diameter $D = 10$ mm.

frequency of resonance that means $f_0 = 3.72$ GHz the effective permittivity of the microstrip line ϵ_{eff} was equal 6.5 and the guided wavelength $\lambda_g = 31.5$ mm. The loaded quality factor $Q_L = 66$, unloaded quality factor Q_U was approximately of 83. The attenuation per guide wavelength α_g , is equal to 0.33 dB/ λ_g

4.2. 1 GHz filter fabrication and measurements

1 GHz bandpass filter was fabricated on the 96% alumina substrate of thickness 0.635 mm in which vias of diameters 1 mm were drilled with a CO_2 laser. On the back side of the substrate the ground plane was screen printed with PdAg conductor while on the upper side the microstrips performing coupling inductors, stub inductors, connecting lines were photoimaged using Fodel Ag 6778. Capacitors were

formed with Fodel dielectric 6050 of dielectric constant $\epsilon_r = 8$. The dielectric layer of thickness 0.042 mm was obtained by the following sequence: (PRINT / DRY / PRINT / DRY / FIRE) x 2.

On the top of the dielectric the upper plates of capacitors were photoimaged with Fodel Ag 6778.

Figure 25 shows SEM photo of the via (x50) in alumina substrate. The via was metallized with PdAg conductor using a miniature small brush rotating at low speed. The filter structure consists of two

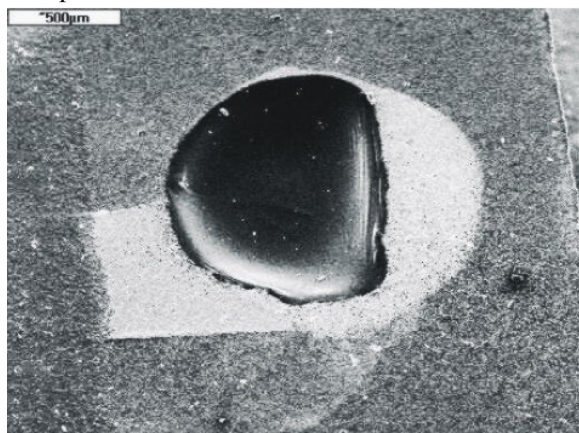


Fig. 25. SEM photo of the via (x50) [7].

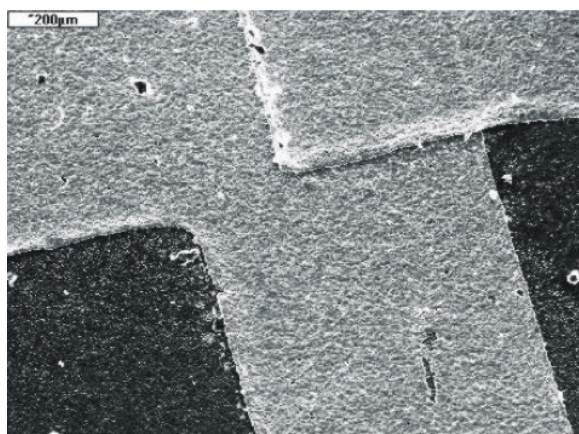


Fig. 26. SEM photo of the connection of two separately performed photoimageable Fodel Ag 6778 layers (x100) [7].

separately performed photoimageable conductor layers and the dielectric layer. Figure 26 shows the area where the upper photoimageable layer connects with the bottom one (x100).

The transmission and reflection characteristics of the 1 GHz filter were measured in a test fixture shown in Fig. 5 in the frequency range from 0.7 GHz to 1.4 GHz with HP 8250C Vector Network Analyzer. The characteristics are shown in Fig. 27a, b.

At the centre of passband that means at 1.05 GHz insertion loss S_{21} was equal -2.13 dB while the return loss S_{11} was equal -12.61 dB. The discrepancy between the design and measurements reveals from two sources: inaccuracy of patterning due to the shrinkage of the layer after firing and the loss of measurement accuracy imposed by the non-ideal terminations. The shrinkage is constant for the given

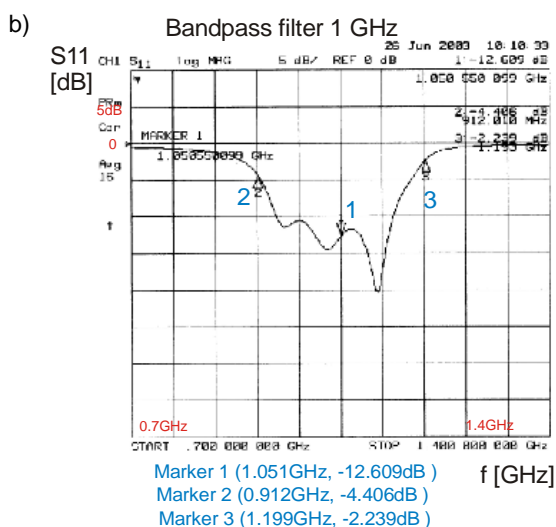
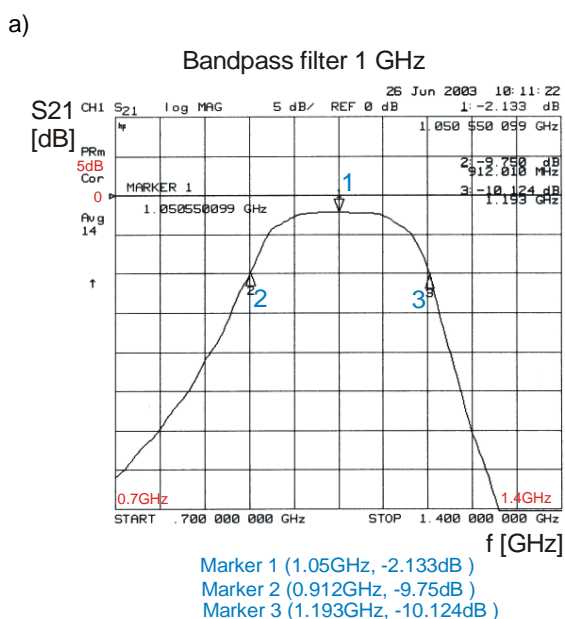


Fig. 27. a) Transmission coefficient S_{21} of the filter 1 GHz, b) reflection characteristic S_{11} of the filter 1GHz.

technological conditions and the proper correction factor introduced at the stage of photomask fabrication is needed to reduce the inaccuracy of patterning. Inaccuracy of measurements requires improvement of matching between the test circuit and the measurement fixture, cables, connectors etc.

4.3. 18 GHz filter fabrication and measurements

Bandpass filter of center frequency 18 GHz is a single layer structure. The microstrip edge-coupled resonators were performed on the top of the 0.635 mm alumina substrate by photoimaging of Fodel 6778. The ground plane was screen printed with PdAg on the opposite side of the substrate.

Table 3 collects the widths of eight gaps between the resonators. The comparison of the designed and real data enables to establish the shrinkage of the layer after firing at the level of 40 μm in each direction.

Table 3. Filter 18 GHz – gap dimensions

Gap	Designed [mm]	Performed [mm]
g_1	0.130	0.219
g_2	0.732	0.803
g_3	1.005	1.082
g_4	1.077	1.164
g_5	1.077	1.156
g_6	1.005	1.081
g_7	0.732	0.813
g_8	0.126	0.211

Figure 28 shows the layout of the microstrip edge-coupled 18 GHz filter.

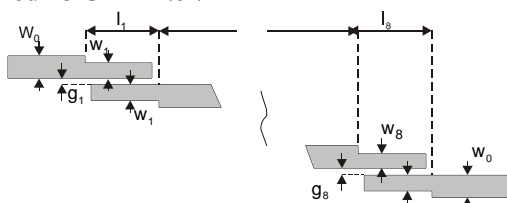


Fig. 28. Layout of the microstrip edge-coupled 18 GHz filter.

Figures 29a, b present the transmission and reflection characteristics of the 18 GHz filter. The filter exhibits in the center of the bandpass at 18.98 GHz the insertion loss S_{21} of 2.94dB.

4.4. Coupler fabrication and measurements

Photoimageable thick film technology is by his nature compatible with the fabrication of multilayer structures. When in a single layer configuration of a microwave circuit very narrow coupling gaps are required which are difficult to obtain even by the most sophisticated photoimaging techniques, the solution is, a double-layer structure where strong capacitive coupling can be accomplished by overlapping the conductor strips deposited on two conductor layers separated by a dielectric sheet [9]. In this latter case the mask aligner is necessary to achieve a correct registration between the dielectric and conductor layers.

The coupler was fabricated on the alumina substrate of thickness $h = 0.635$ mm and relative permittivity $\epsilon_r = 9.6$. Fodel dielectric 6050 of thickness $t = 0.12$ mm and relative permittivity $\epsilon_r = 8$ was deposited in the coupling area between two overlapped microstrips. The structural dimensions of a coupler have been determined as $w_1 = 0.25$ mm (bottom microstrip width), $w_2 = 0.40$ mm (upper microstrip width), $S = 0.12$ mm and $L = 4$ mm. The connecting output lines of $Z_0 = 50 \Omega$ characteristic impedance were used.

On the backside of the alumina substrate of thickness 0.635 mm the ground plane was screen

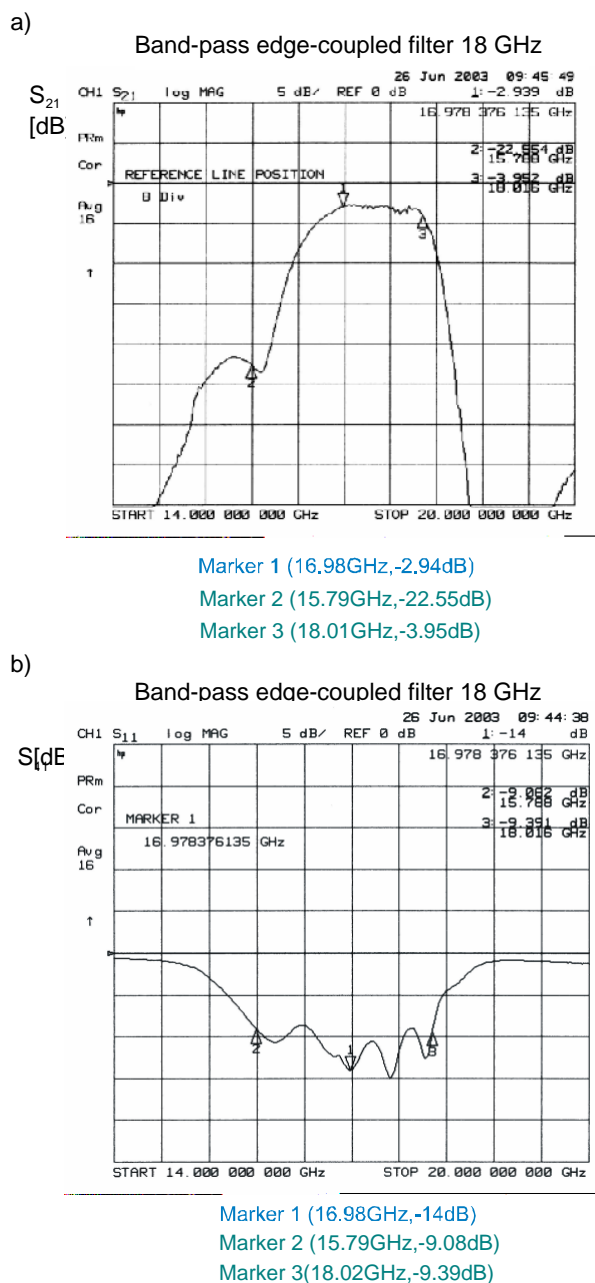


Fig. 29. a) Transmission characteristic S_{21} of the 18 GHz filter, b) reflection characteristic S_{11} of the 18 GHz filter.

printed with PdAg conductor. On the other side of the substrate the lower coupling microstrip of width 0.250 mm and length 3 mm as well as connecting lines were photoimaged using Fodel Ag 6778 conductor. Afterwards in the coupling area, the Fodel 6050 dielectric layer of final thickness 0.120 mm was deposited by the following process:

(PRINT / DRY / PRINT / DRY / FIRE) x 3.

At the top of the dielectric layer the upper coupling microstrip of width 0.400 mm and length 4 mm was photoimaged with Fodel Ag 6778. Figure 30 shows the upper microstrip flowing down the dielectric slope and connecting with the line beneath on the alumina substrate.

To measure the full four-port characteristics of the coupler, 50 Ω terminations were used to match the unmeasured ports of a test circuit. The measured

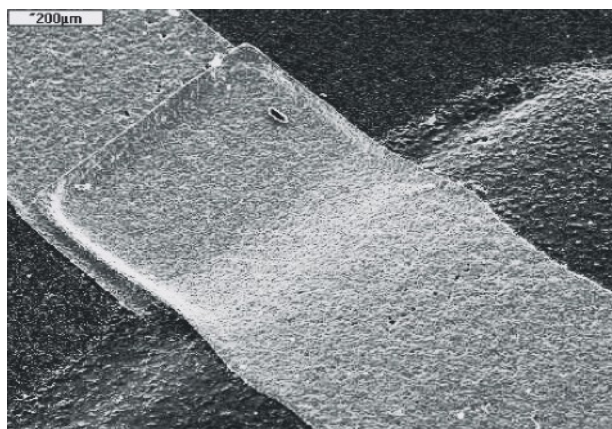


Fig. 30. Insertion loss S_{21} and coupling S_{31} of the coupler in the frequency range 1 GHz to 18 GHz.

insertion loss S_{21} and coupling response S_{31} of the coupler in the frequency range 1 GHz to 18 GHz are plotted in Fig. 31. At 7.5 GHz the measured insertion loss S_{21} of the coupler is -4.2 dB and the coupling response S_{31} is -6 dB, respectively. The insertion loss S_{21} characteristic and the coupling S_{31} characteristic

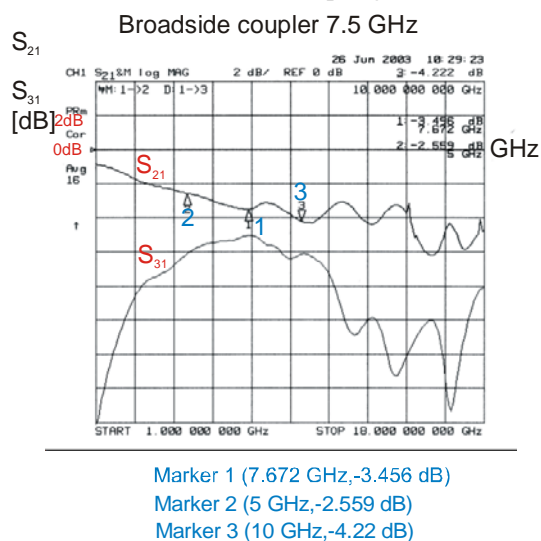


Fig. 31. Insertion loss S_{21} and coupling S_{31} of the coupler in the frequency range 1 GHz to 18 GHz.

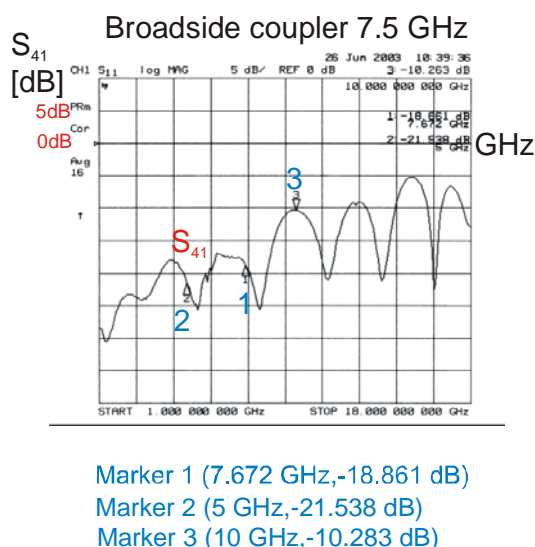


Fig. 32. Isolation S_{41} of the coupler.

do not cross that means that coupling between microstrips situated at the bottom and at the top of Fodel dielectric is too weak. It is supposed that the dielectric layer is simply too thick and further works are planned to improve the coupling. The measured isolation response S_{41} of the coupler is plotted in Fig. 32. At 7.5 GHz the measured isolation response S_{41} is -14 dB comparing to the simulated one equal -14.1 dB and shows quite good agreement.

5. Conclusions

It has been shown some potential of the photoimageable thick-film technology in fabricating single- and double-layer microwave circuits such as ring resonators, bandpass filters and couplers. Novel construction of development unit with application of ultrasonic generators has been presented and applied for photoimaging thick-films.

The results demonstrated that thick-film photoimageable technology is well suited to fabrication of low-loss, low cost and high-performance microwave circuits.

Further works are planned to eliminate discrepancies between measured and simulated responses.

REFERENCES

1. DuPont Data Sheets: www.dupont.com/mcm/
2. M. TREDINNICK, P. BARNWELL, D. MALANGA, *Thick-Film Fine Line Patterning – A Definite Discussion of the Alternatives*, 2001 Int. Symp. on Microelectronics, Baltimore, USA, 9–11.10.2001, 679–681.
3. P. BARNWELL, *Ceramic Circuitry– A Technology for the Future*, 38th IMAPS Nordic Conf., Oslo, Norway, 2001, 8488.
4. Z. TIAN, Ch. FREE, C. AITCHISON, P. BARNWELL, J. WOOD, *Multi-Layer Thick-Film Microwave Components and Measurement*, Microelectron. Int. 2003, **20**, 1, 7–20.
5. B. DZIURDZIA, Z. MAGOŃSKI, M. CIEŻ, W. GREGORCZYK, *Thick-Film Photoimageable Conductor and Dielectric in Microwave Circuits*, 48 Int. Wissenschaft Kolloq. Technische Universität Ilmenau, Germany, 22–25.09.2003.
6. J. CRUTE, L. DAVIS, *Loss Characteristics of High ϵ_r Microstrip Lines Fabricated by an Etchable Thick-Film on Ceramic MCM Technology*, IEEE Trans. on Adv. Packag., 2002, **25**, 3, 393–396.
7. B. DZIURDZIA, S. NOWAK, Z. MAGOŃSKI, M. CIEŻ, W. GREGORCZYK, W. NIEMYJSKI, *On the Design and Fabrication of Photoimageable Thick-Film Multilayer Filters and Couplers*, 27th Int. Conf. a. Exhib. IMAPS-Poland 2003, Podlesice, 16–19.09.2003, 143–149.
8. B. DZIURDZIA, Z. MAGOŃSKI, M. CIEŻ, W. GREGORCZYK, *Photoimageable Dielectric-Processing, Properties, Compatibility with Conventional Thick-Film Conductors*, 26th Int. Conf. a. Exhib. IMAPS-Poland 2002, 25–27.09.2002, Warszawa, Poland, 134–141.
9. W. MARCZEWSKI, NIEMYJSKI W., *The Overlapped Microstrip Lines for MICs and MMICs*, 14th Europ. Microwave Conf., Liege, Belgium, Sept. 1984.